

BOND PERFORMANCE OF DEFORMED REBAR IN STEEL FIBER REINFORCED LIGHTWEIGHT-AGGREGATE CONCRETE AFFECTED BY MULTI-FACTORS

Mingshuang Zhao¹, Xiaoyan Zhang², Kai Yan¹, Teng Fei¹, Shunbo Zhao¹

1. Henan Province International United Lab of Eco-building Materials and Engineering, North China University of Water Resources and Electric Power, No. 36 Beihuan Road, 450045 Zhengzhou, China; E-mail: 1287827643@qq.com (Mingshuang Zhao), 1743767554@qq.com (Yan), 1751447427@qq.com (Fei), sbzhao@ncwu.edu.cn (Shunbo Zhao)
2. School of Civil Engineering and Communication, North China University of Water Resources and Electric Power, No. 136 Jinshui East Road, 450046 Zhengzhou, China; E-mail: zxyanzi@ncwu.edu.cn

ABSTRACT

For the innovation of building materials, a new high-performance Steel Fiber Reinforced Lightweight-Aggregate Concrete (SFRLAC) made of 100% fine and coarse expanded shales has been developed. In view of the importance of reliable bond properties between deformed rebar and this new SFRLAC, the experimental study of 39 specimens was conducted by using the modified pull-out test method with the evaluation of different slips at loading-end and free-end. In which the influencing factors were considered as the volume fraction of steel fiber, the water-cement ratio, the rebar diameter, the bond length of rebar, the strength of coarse expanded shales and the fine expanded shale replaced by manufactured sand. The complete bond stress-slip curves were measured, the bond failure modes of specimens were observed. Based on the bond mechanism of adhesion, friction and bearing action of deformed rebar in SFRLAC, the bond performance characterized by the bond strength and peak-slip, the differential of bond slip between loading-end and free-end, the bond sustainability in descending portion and the bond failure mode observed are analyzed. The recommendations are proposed for the design of SFRLAC structures related to the bond performance.

KEYWORDS

Steel fiber reinforced lightweight-aggregate concrete, Bond performance Modified pull-out test, Bond stress-slip curve, Bond strength, Peak-slip, Bond sustainability

INTRODUCTION

As a green building materials, lightweight-aggregate concrete (LAC) has been applied in civil engineering to lighten the self-weight of building structures and get other benefits such as better earthquake resistance and thermal insulation [1, 2]. However, owing to the different lightweight aggregates such as expanded clay aggregate, expanded shale aggregate, cold-bonded fly ash aggregate, sintered pulverized fuel ash aggregate, pelletized blast furnace slag aggregate, pumice aggregate, oil palm shell aggregate, etc., the properties of LAC may be varied in a great extent [3, 4]. In aspect to utilize the local expanded shale as lightweight aggregate, a new LAC dealt with 100% expanded shales as fine and coarse aggregates was innovated. Experimental

studies on the basic mechanical properties [5-7], strength development and carbonation [8], and shrinkage [9] of this LAC mixed with steel fibres were finished, and a new Steel Fiber Reinforced Lightweight-Aggregate Concrete (SFRLAC) with high structural performances was developed [10-12].

For the structural application, the bond performance of rebar in this new SFRLAC is important to ensure their working together. Similar to the reports about the bond properties of plain rebar in LAC [13], two kinds of actions affect the bond performance between plain rebar and this new SFRLAC: the adhesion referred to the chemical bonding of set cement is dominant before the bond stress reaches the ultimate; after that, the friction arising from the roughness of the interface becomes control. From the bonding mechanism, both the adhesion and the friction rely on the strength of set cement adhered on the interface. Therefore, the bond stress-slip behaviour is affected obviously by the water-binder ratio, and the bond strength increases mainly with the decrease of water-binder ratio. The bond strength trends a slight increment with the increasing volume fraction of steel fiber, while the bond sustainability rises after the peak-slip in descending portion of bond stress-slip curve. Meanwhile, the bond performance is less influenced by the strength of coarse expanded shale and the different fine aggregates tested [14].

As the deformed rebar is popular used for the main reinforcement, the bond performance of deformed rebar in this new SFRLAC should also be reasonably evaluated. In this respect, the studies on bond properties of LAC dealt with expanded shale provide good references [15-22], and the enhancement of steel fibres on the bond of SFRLAC presents a bright prospect [23-27].

Except the adhesion and friction on bond interface, the bearing action due to the anchorage of ribs against LAC surface benefits much more to the bond between deformed rebar and LAC [1, 13]. As the rib surface is not perpendicular to the longitudinal axis of rebar, the bearing action is resulted from the comprehensive effects of LAC under compression, tension and shear. Therefore, the issues were focused on the types of lightweight-aggregate and the strength of LAC (or water-binder ratio). Clarke and Birjandi [15] did not observe significant difference in the bond strengths of LAC using coarse expanded shale and other coarse lightweight aggregates such as expanded clay and pelletized blast furnace slag aggregates. Konig *et al.* [16] found higher bond strength of LAC with coarse expanded shale compared to the LAC with coarse expanded clay due to the higher compressive and splitting tensile strength of the former LAC. Lachemi *et al.* [17] reported that under the conditions of equivalent workability and compressive strength, the bond properties of LAC with coarse expanded shale was significantly enhanced compared to the LAC with coarse lightweight slag aggregate. Wu *et al.* [18] reported that the LAC with coarse expanded shale exhibited higher bond strength compared to the LAC with sintered pulverized fuel ash aggregate when equal water-binder ratio was used for both mixes. Meanwhile, the bond strength between deformed rebar and LAC with coarse expanded shale increases with the increasing tensile and/or compressive strength of LAC [19-22], and is higher than that of ordinary concrete in the same strength grade due to the lower water-binder ratio of LAC [19, 20].

Regardless of types of coarse lightweight-aggregate used such as cold-bonded fly ash, expanded clay, oil palm shell and expanded shale aggregates, the addition of steel fiber enhances the bond strength of deformed rebar in SFRLAC. This may be due to the increased confinement effect which altered the failure mode from splitting to pull-out failure [23], the bridging effect of steel fiber which restrained the widening of cracks appeared on surface of SFRLAC to improve the splitting failure [24, 25], or the strengthening effect which arrested the propagation of internal micro-cracks in pull-out failure [25]. The enhancements depend on the different conditions of concrete cover, rebar diameter, volume fraction of steel fiber and strength of SFRLAC. Meanwhile, Zhang *et al.* [26] observed that the peak-slip increased slightly with the increasing volume fraction of steel fiber, while the bond-stress in descending portion reduced slowly with higher loading resistance. Mo *et al.* [27] reported that the peak-slip increased with the increasing volume fraction

of steel fiber, while the bond stress-slip curve did not affected.

Given above, the bond performances of deformed rebar in SFRLAC are not fully recognized. This leads to the specially focuses on the bond performance of deformed rebar in the new high-performance SFRLAC in this paper. In the experimental study, the effects of such factors as the volume fraction of steel fiber, the water-cement ratio, the rebar diameter, the bond length of rebar, the strength of coarse expanded shales and the fine expanded shale replaced by manufactured sand were considered. The complete bond stress-slip curves and bond failure modes are measured by using the modified pull-out test method. Based on the analyses of test results, some beneficial recommendations are proposed for the safeguard design relating to the bond of high-performance SFRLAC structures.

EXPERIMENT

Raw materials

Grade P.O. 42.5 ordinary silicate cement was used, the physical and mechanical properties are listed in Table 1. Two kinds of sintering expanded shale in continuous gradation with maximum size of 20mm were used as coarse aggregate which sieved based on the maximum density principle, their physical and mechanical properties are presented in Table 2. The fine aggregate was the lightweight fine sintering expanded shale and the manufactured sand respectively in continuous gradation with size of 1.6-5 mm, their physical properties are listed in Table 3. Meanwhile, Table 4 presents the tested water absorption of coarse and fine expanded shales.

Tab. 1 - Physical and mechanical properties of cement

Strength grade	Water requirement of normal consistency (%)	Setting time (min)		Compressive strength (MPa)		Tensile strength (MPa)	
		initial	final	3d	28d	3d	28d
42.5	26.4	150	248	22.8	50.8	4.1	8.0

Tab. 2 - Physical and mechanical properties of expanded shale

Identifier	Apparent density (kg/m ³)	Bulk density (kg/m ³)	1h water absorption (%)	Mud content (%)	Cylinder compressive strength (MPa)
N	1274	800	6.1	0.2	5.0
H	1471	917	6.5	0.2	6.2

Tab. 3 - Physical properties of lightweight sand and manufactured sand

Identifier	Fineness modulus	Apparent density (kg/m ³)	Bulk density (kg/m ³)	1h water absorption (%)	Mud content (%)	Stone powder (%)
L	3.56	1659	946	9.0	1.5	-
M	2.50	2730	1930	0.90	-	7.9

Tab. 4 - Water absorption of aggregate with the change of time

Aggregate	Term	5 min	10 min	15 min	30 min	1 h
Expanded shale	Absorption (%)	4.0	5.0	5.2	5.5	6.1
	Relative to 1 h (%)	65.6	82.0	85.2	90.2	100
Lightweight sand	Absorption (%)	8.0	8.4	8.7	8.8	9.0
	Relative to 1 h (%)	89.2	93.4	96.8	98.1	100

Steel fiber was milling type in length $l_f=30$ mm and equivalent diameter $d_f=0.8$ mm. The aspect ratio $l/d_f=37.5$. Others were the tap-water and the polycarboxylic acid superplasticizer with water-reducing rate of 19 %.

Mix proportion of SFRLAC

The variables of this study were considered as the volume fraction of steel fiber (ρ_f), the water-cement ratio (W/C), the strength of coarse lightweight aggregate and the type of fine aggregate. Table 5 lists their combinations, where the double letters of mix No. are the identifiers of expanded shale and fine aggregate, the following digits represent W/B and ρ_f .

The mix proportion of high-performance SFRLAC was designed in accordance with the specifications in China Standards [28, 29], where the absolute volume method was selected. For all mixes, the dosage of water reducer was 5.5 % cement in mass. All mixes had good workability with slump of 120mm~150mm.

Tab. 5 - Mix proportion, compressive and tensile strength of concrete

Mix No.	W/C	Cement (kg/m ³)	Water (kg/m ³)	Steel fiber (kg/m ³)	Sand (kg/m ³)	Expanded shale (kg/m ³)	f_{cu} (MPa)	f_{ft} (MPa)
NL0.30/0	0.30	460	138	—	491.1	519.8	41.7	1.59
NL0.30/0.4	0.30	487	147	31.2	484.4	508.6	44.1	2.03
NL0.30/0.8	0.30	513	155	62.4	478.7	497.5	46.4	2.23
NL0.30/1.2	0.30	541	164	93.6	472.4	485.7	47.3	2.81
NL0.25/0.8	0.25	543	136	62.4	466.2	526.8	50.4	2.49
NL0.35/0.8	0.35	483	169	62.4	499.4	477.9	44.4	1.87
NM0.30/0.8	0.30	513	155	62.4	787.7	497.5	59.2	2.15
HL0.30/0.8	0.30	513	155	62.4	478.7	574.4	58.5	2.77

Preparation of specimens

The bond behaviour of deformed rebar in high-performance SFRLAC was experimented by using the modified central pull-out test method [30-32]. The deformed rebar was steel bar with crescent-ribs. Table 6 lists their mechanical properties.

Tab. 6 - Mechanics properties of rebar

Type	d (mm)	Yield strength (MPa)	Ultimate tensile strength (MPa)	Fracture elongation (%)
HRB335	12	365	565	21.2
HRB335	16	371	561	23.9
HRB335	20	375	563	24.6

The bond length of rebar was placed in the central part of specimen with the bond-breakers in length of 35 mm at the ends. Realized by PVC tubes and sealed with paraffin, the bond-breakers simulated the real condition of rebar in concrete, and eliminated the local compression on loading surface. The normal section of specimen was 150 mm×150 mm, the bond length of rebar $l_a=2d$, $5d$, $8d$ and $11d$ (where d is rebar diameter), the length of specimen $l=l_a+70$, the steel bar at loading end was kept long enough for pull-out purpose. Thirteen groups of specimen were designed, each group had 3 specimens. The group No. means the variables of bond length, rebar diameter followed by mix No. (Table 7).

Tab. 7 - List of specimens

Group No.	Mix No.	ρ_x (%)	d (mm)	l_a (mm)	l (mm)	Aggregates
5d16NL0.30/0	NL0.30/0	0	16	80	150	N+L
5d16NL0.30/0.4	NL0.30/0.4	0.4	16	80	150	N+L
5d16NL0.30/0.8	NL0.30/0.8	0.8	16	80	150	N+L
5d16NL0.30/1.2	NL0.30/1.2	1.2	16	80	150	N+L
5d16NL0.25/0.8	NL0.25/0.8	0.8	16	80	150	N+L
5d16NL0.35/0.8	NL0.35/0.8	0.8	16	80	150	N+L
5d16HL0.30/0.8	HL0.30/0.8	0.8	16	80	150	H+L
5d16NM0.30/0.8	NM0.30/0.8	0.8	16	80	150	N+M
5d12NL0.30/0.8	NL0.30/0.8	0.8	12	60	130	N+L
5d20NL0.30/0.8	NL0.30/0.8	0.8	20	100	170	N+L
2d16NL0.30/0.8	NL0.30/0.8	0.8	16	32	102	N+L
8d16NL0.30/0.8	NL0.30/0.8	0.8	16	128	198	N+L
11d16NL0.30/0.8	NL0.30/0.8	0.8	16	176	246	N+L

The specimens were prepared and cured in the lab. Steel moulds with holes at central of opposite plates ensured the placement of rebar [32]. The SFRLAC was put into the moulds and vibrated on the vibration platform. After cast for 24 hours, the specimens were moved from moulds and placed in the standard curing room for 28 days. To get the real compressive and tensile strengths of SFRLAC, six cubes in dimension of 150 mm for each mix were cast at the same time and cured in the same condition with specimens.

Test Method

On test platform, the loading-end of rebar passed successively through the steel plate, steel tube, load meter and locked at the end of hydraulic jack. All of them fixed together were adjusted with the axis of rebar to eliminate the eccentric effect of pull-out force. The bond slip at loading-end was measured by the displacement meter fixed on the rebar within the steel tube, which was corrected by accounting for the local elongation of the rebar. The slip at free-end was accounted by the relative displacement between rebar and concrete measured with two displacement meters. The displacement meters linked to the strain acquisition system. The initial load was exerted on the specimen to check the stability of test system, and then the static loading test was started. As specified in China Standard [30], the loading speed changes with different diameter (d) of steel bar, it was taken as $0.05d^2$ N/min.

The average bond stress (τ) was calculated from the pull-out force divided by the bond area within bond length, the maximum value was the bond strength (τ_u), that is:

$$\tau = F / (\pi d l_a) \quad (1)$$

Where, F is the pull-out force, l_a is the bond length of rebar, d is the diameter of rebar.

Tests for cubic compressive strength (f_{cu}) and splitting tensile strength (f_t) of SFRLAC were in accordance with the specifications of China Standard [33]. The results are presented in Table 5.

TEST RESULTS AND DISCUSSION

Failure states, bond strength & peak-slip

Except those specimens with $11d$ bond length failed due to the yield of rebar without pull-out from the SFRLAC, the LAC specimens (5d16NL0.30/0) failed due to the splitting of LAC after the pull-out load reached the maximum, while the others of SFRLAC specimens failed because of the pull-out of rebar accompanied with cracks appeared on side surfaces of SFRLAC. Therefore, the bond stress-slip curves of LAC specimens were obtained only before ultimate load, while the complete bond stress-slip curves of SFRLAC specimens were gotten.

Steel fibres protected the splitting of SFRLAC specimens into two or three parts as those of LAC, which led a ductile bond failure due to the successive pull-out of rebar. As the slip of rebar gradually transferred from loading-end to free-end, the loading-end slip was larger than the free-end slip until the pull-out load up to the maximum. After that, the increments of slip at free-end and loading-end were almost equal. During the pull-out process of rebar, cracks appeared and widened continuously on the side surface of SFRLAC specimens. With the increasing volume fraction of steel fiber, the crack width decreased due to the enhanced confinement of steel fibres on crack widening. Table 8 lists the maximum crack width measured on the side surface of specimens while the rebar was fully pull out of SFRLAC.

From the bond stress-slip curve, the maximum bond stress is the bond strength (τ_u), and the corresponding peak-slip is marked as s_u . Table 9 lists test values of the bond strength (τ_u) and the peak-slips at free-end ($s_{f,u}$) and loading-end ($s_{l,u}$). The mean values are computed for the specimens failed without yield of rebar according to the statistical analysis principle of the deviation within 20 %. The value of peak-slip (s_u) is taken as the mean value of peak-slips at free-end and loading-end, to generally analyse the bond stress-slip relationship.

Tab. 8 - Maximum crack width appeared on side surface of specimen (mm)

Group no.	Specimen no.		
	1	2	3
5d16NL0.30/0.4	3.50	3.30	2.00
5d16NL0.30/0.8	2.00	2.50	1.10
5d16NL0.30/1.2	1.50	0.38	0.45

Tab. 9 - Test result of bond strength and slip

Group no. of specimens	τ_u (MPa)		$s_{l,u}$ (mm)		$s_{f,u}$ (mm)		s_u (mm)	Failure mode*
	test value	mean	test value	mean	test value	mean		
5d16NL0.30/0	14.5/13.2/14.0	13.9	0.37/0.35/0.38	0.37	0.26/0.27/0.28	0.27	0.32	S/S/S
5d16NL0.30/0.4	15.5/16.5/14.5	15.5	0.74/0.86/0.68	0.76	0.50/0.60/0.54	0.55	0.66	P/S/P
5d16NL0.30/0.8	17.0/16.1/17.7	16.9	1.06/0.91/0.94	0.97	0.57/0.51/0.54	0.54	0.76	P/P/P
5d16NL0.30/1.2	18.9/19.8/19.1	19.3	1.19/1.13/1.16	1.16	0.41/0.38/0.40	0.40	0.78	P/P/P
5d16NL0.25/0.8	18.5/18.3/19.1	18.6	1.08/0.94/1.05	1.02	0.46/0.50/0.45	0.47	0.75	S/P/P
5d16NL0.35/0.8	15.1/17.4/16.5	16.3	0.85/0.93/0.96	0.91	0.62/0.60/0.64	0.62	0.77	P/S/P
5d16HL0.30/0.8	17.5/19.1/17.8	18.1	1.05/1.01/1.01	1.02	0.48/0.40/0.46	0.45	0.74	S/P/P
5d16NM0.30/0.8	17.3/16.3/16.5	16.7	0.62/0.61/0.67	0.63	0.55/0.60/0.56	0.57	0.60	P/P/P
5d12NL0.30/0.8	17.8/16.7/17.5	17.3	0.78/0.79/0.90	0.82	0.49/0.52/0.55	0.52	0.67	P/P/P
5d20NL0.30/0.8	15.1/16.5/17.2	16.3	0.72/0.79/0.71	0.74	0.53/0.50/0.61	0.55	0.65	P/S/S
2d16NL0.30/0.8	17.0/15.7/17.5	16.7	0.58/0.60/0.55	0.58	0.44/0.46/0.52	0.47	0.53	P/P/P
8d16NL0.30/0.8	13.2/12.6/12.9	12.9	1.20/1.19/1.21	1.20	0.35/0.33/0.40	0.36	0.78	P/S/S

Note: *S-splitting of LAC or SFRLAC; P-pull-out of rebar.

Effect of steel fibres

As shown in Figure 1, the bond stress-slip (τ - s) curves of rebar pull-out of SFRLAC contain three portions with the characteristics of micro-slip, slip and descending. In the micro-slip portion, the slip increased elastically due to the continuous loss of adhesion between rebar and SFRLAC. In the slip portion, the bond stress increased nonlinearly with slip as the SFRLAC in front of the ribs of rebar became into the nonlinear deformation under compression, tension and shear. Accompanied with the internal broken of SFRLAC in front of the ribs of rebar, the splitting cracks appeared on the side surface of specimen, the bond stress reached the ultimate with the peak-slip, and the bond stress-slip curve went into the third portion.

Similar to the reported study [26, 27], due to the restraint of steel fibres to the propagation of internal cracks of SFRLAC, the slip of rebar kept persistently with the successive shear fracture and compressive broken of SFRLAC along the rebar.

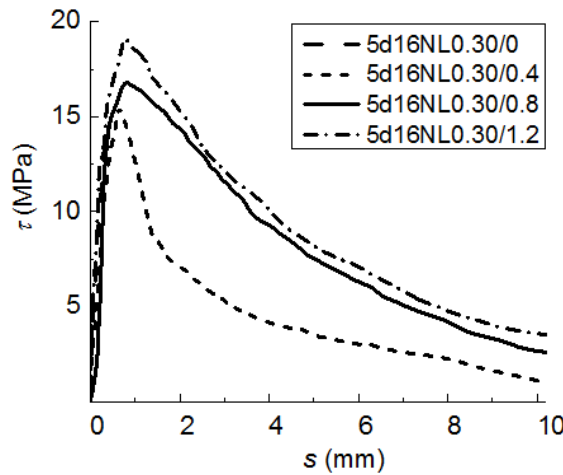


Fig. 1 - Bond stress-slip curves of specimens with different volume fraction of steel fiber

Normally, the bond strength (τ_{u0}) between deformed rebar and LAC is expressed as a function of compressive strength (f_{c0}) or tensile strength (f_{t0}) of LAC [13, 17, 19], which can be generally shown as:

$$\tau_{u0} = a f_{c0}^b \tag{2}$$

$$\tau_{u0} = c f_{t0} \tag{3}$$

Where a , b and c are the fitness coefficients depended on the test parameters.

Considering that the tensile strength (f_{ft}) of SFRLAC is always expressed as linearly to the content characteristic value (λ_f) of steel fiber, that is [7, 10, 29]

$$f_{ft} = (1 + \alpha_t \lambda_f) f_{t0} \tag{4}$$

Where α_t is the fitness coefficient. $\lambda_f = \rho_f \cdot k / d_f$, ρ_f is the volume fraction of steel fiber, k/d_f is the aspect ratio of steel fiber.

Suppose Equation 3 is also fit for the bond strength (τ_u) between deformed rebar and SFRLAC, the following equation can be deduced as:

$$\tau_u = (1 + \alpha_b \lambda_f) \tau_{u0} \tag{5}$$

The reasonability of Equations 4 and 5 can be verified by the test results shown in Figure 2. Where the tensile strength ratio, bond strength ratio and compressive strength ratio are f_{ft}/f_{t0} , τ_u/τ_{u0} and f_{cd}/f_{c0} , respectively. Obviously, the increment of bond strength is lower than that of tensile strength with the same increment of the volume fraction of steel fiber. The addition of 0.4%, 0.8% and 1.2% steel fibres resulted in increase of 11.5%, 21.6% and 38.9% in the bond strength of SFRLAC, while the increase of 27.6%, 40.2% and 76.7% in the tensile strength. This means the coefficient $\alpha_b < \alpha_t$, and explains that the enhancement of steel fibres on bond strength not only depended on the strengthening of tensile strength, but also on the compressive strength. The less strengthening of compressive strength reduced the resistance of SFRLAC in front of the ribs of rebar under compression. In this aspect, Equation 2 has certain reasonability reflecting the comprehensive effect of LAC strength on bond strength by using the exponential function of compressive strength.

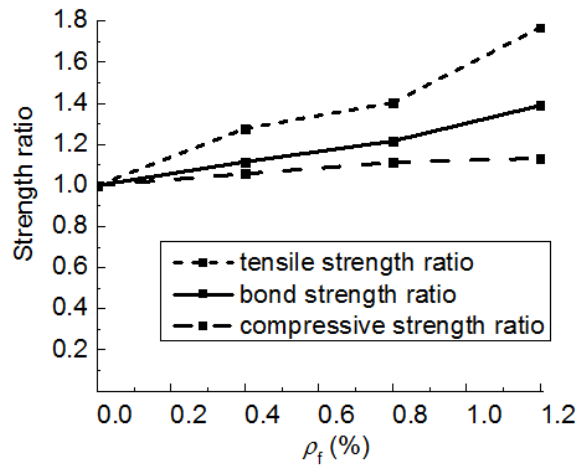


Fig. 2 - Bond strength affected by the volume fraction of steel fibres

Figure 3 shows that with the increasing volume fraction of steel fiber, the mean values of peak-slip (s_u) were almost equal, however the slip at loading-end increased and the slip at free-end became smaller, which resulted in the increased deviation of slips at loading-end and free-end. This illustrates that the steel fibres in SFRLAC restrained the internal splitting of SFRLAC along rebar and led to the continuously increment of bond stress from loading-end to free-end [31, 32], resulted in the enhancement of the sustainability of bond between deformed rebar and SFRLAC.

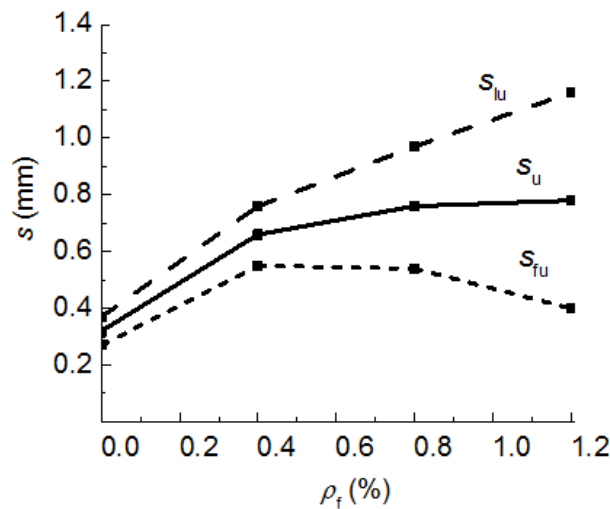


Fig. 3 - Bond slip affected by the volume fraction of steel fibres

In this paper, the bond sustainability of deformed rebar in SFRLAC is in direct proportion to the normalized bond stress τ_r/τ_u . Where τ_r is the bond stress at point of bond stress-slip curve in descending portion, normally called as residual bond strength. As shown in Figure 4, when the same slip took place in descending portion of bond stress-slip curve, τ_r/τ_u was higher with the volume fraction of steel fiber no less than 0.8 %. This result is different from Mo *et al.* reported [27] that the addition of steel fiber did not affect the bond stress-slip curve, where the oil palm shell was used as coarse lightweight-aggregate. With the lower volume fraction of steel fiber as 0.4%, the bond sustainability was poor although the brittleness of bond failure was improved obviously.

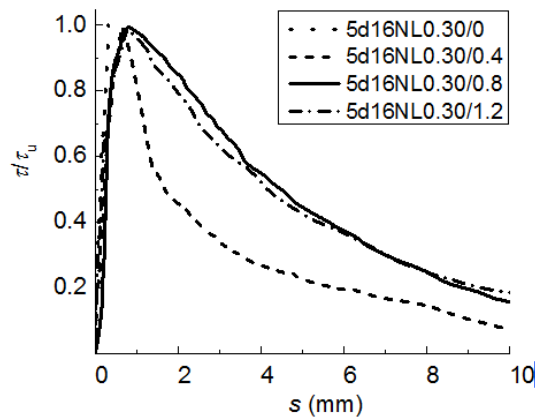


Fig. 4 - Bond sustainability affected by the volume fraction of steel fibres

Effect of SFRLAC strength

In the test, the different of SFRLAC strength depended on the different water-cement ratio. From Table 5, the compressive and splitting tensile strengths of SFRLAC increased with the decrease of water-cement ratio. This provided the good condition to enhance the bond performance of deformed rebar in SFRLAC. As listed in Table 9, the bond strength increased with the decreasing water-cement ratio, the differential of slips at loading-end and free-end become larger in spite of the almost equal mean value of peak-slip. More directly, Figure 5 presents the increasing trend of bond performance with the decrease of water-cement ratio.

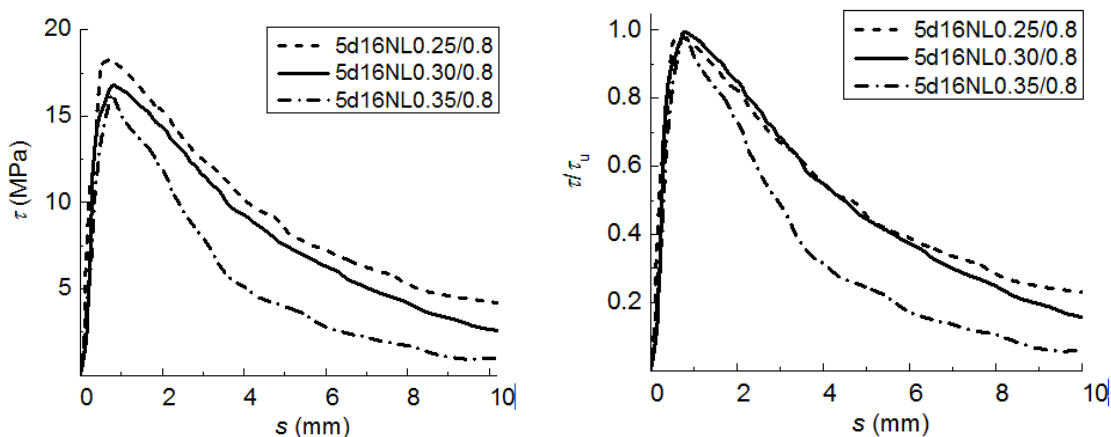


Fig. 5 - Bond stress-slip curve and bond sustainability affected by the water-cement ratio

Figure 5 also shows the bond sustainability of SFRLAC with different water-cement ratio. Due to the complex action of SFRLAC under compression and shear in front of ribs and along bond length of rebar, the bond sustainability was almost equal when the water-cement ratio was 0.25 and 0.30, while the lower bond sustainability was for the water-cement ratio of 0.35.

Effect of rebar diameter

From Table 9, the bond strength reduced slightly with the increase of rebar diameter, the mean value of peak-slip decreased with the reduced differential of peak-slips between loading-end

and free-end. Compared the bond strength of rebar $d=12\text{mm}$, the bond strength of rebar $d=16\text{mm}$ and 20mm decreased for 2.31% and 5.78%. From Figure 6, the bond stress of rebar $d=20\text{mm}$ drop down quickly with the increased slip in descending portion of bond stress-slip curve, which was bad for the bond sustainability. These may be due to the reduction of bearing capacity of SFRLAC in front of ribs, as the height of ribs relatively reduced and the space of ribs increased with the increasing diameter of rebar [1, 2]. Another reason may be owing to the changes of concrete cover from 5.75, 4.19 to 3.25 times the rebar diameter, which led to the increasing trend of the splitting failure of SFRLAC and decreased the lateral restraint to the bond surface. Similar regulations of bond strength of LAC reduced with the increasing rebar diameter are reported in previous studies [16-20]. As the proof, two of three specimens with 20mm rebar failed in splitting of SFRLAC in this test.

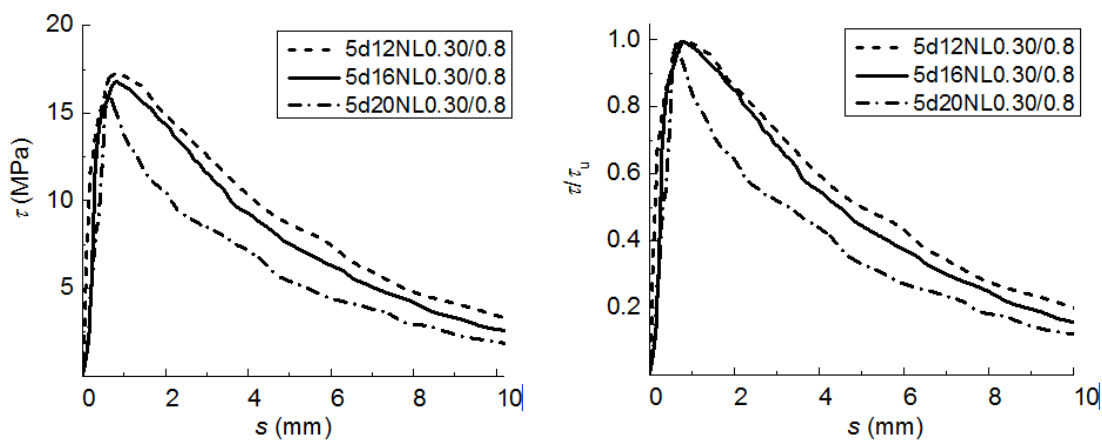


Fig. 6 - Bond stress-slip curves and bond sustainability affected by diameter of rebar

Effect of aggregate types

The SFRLAC (HL0.30/0.8) with higher strength expanded shale had greater compressive and tensile strengths than the SFRLAC (NL0.30/0.8) with normal strength expanded shale (Table 5). This resulted in the higher bond strength, the larger differential of peak-slip between loading-end and free-end (Table 9) and the relative fullness of bond stress-slip curve (Figure 7). Taken an observation on the failure of bond interface, the expanded shales were directly sheared as a plain. This demonstrated that the strength of expanded shales played an important role resisting the complex action under shear and compression.

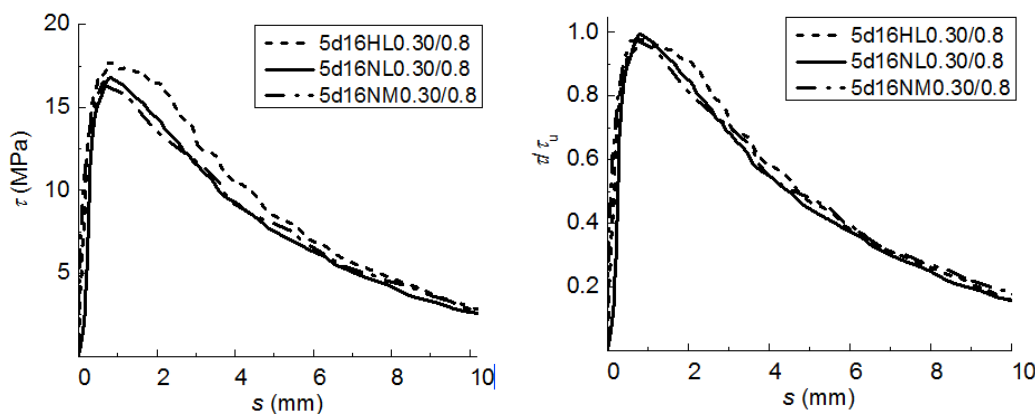


Fig. 7 - Bond stress-slip curves affected by types of coarse and fine aggregates

The SFRLAC (NM0.30/0.8) with manufactured sand had greater compressive strength and slightly lower tensile strength than the SFRLAC (NL0.30/0.8) with normal strength expanded shale (Table 5). This resulted in the almost equal bond strength with some differential of slip (Table 9), and the similar bond stress-slip curve and bond sustainability (Figure 7).

Therefore, the strength of coarse expanded shale affected the bond performance in much more extent, while the effect of fine expanded shale replaced by manufactured sand could be eliminated.

Effect of bond length

With the increase of bond length, the pull-out load increased. This led to the increase of tensile stress of rebar over the yield strength as well as ultimate strength, and finally resulted in the fracture of rebar when the bond length reached $11d$. Combined with test data in Table 9 and bond stress-slip curves in Figure 8, the bond strength of rebar with $2d$ bond length was equal to that with $5d$ bond length, while the bond strength of rebar with $8d$ bond length was lower about 30%. The fullness of bond stress-slip curve in descending portion of rebar with $2d$ bond length was better than those of rebars with $5d$ and $8d$ bond length. The rebars with $5d$ and $8d$ bond length presented the similar bond stress-slip curve and bond sustainability, although the latter has a greater differential of peak-slips between loading-end and free-end. Meanwhile, it should be noted that the bond sustainability of rebar with $8d$ bond length at the initial part of descending portion of τ/τ_u - s curve was greater, which provided a higher reliability to sustain the bond strength with a greater peak-slip.

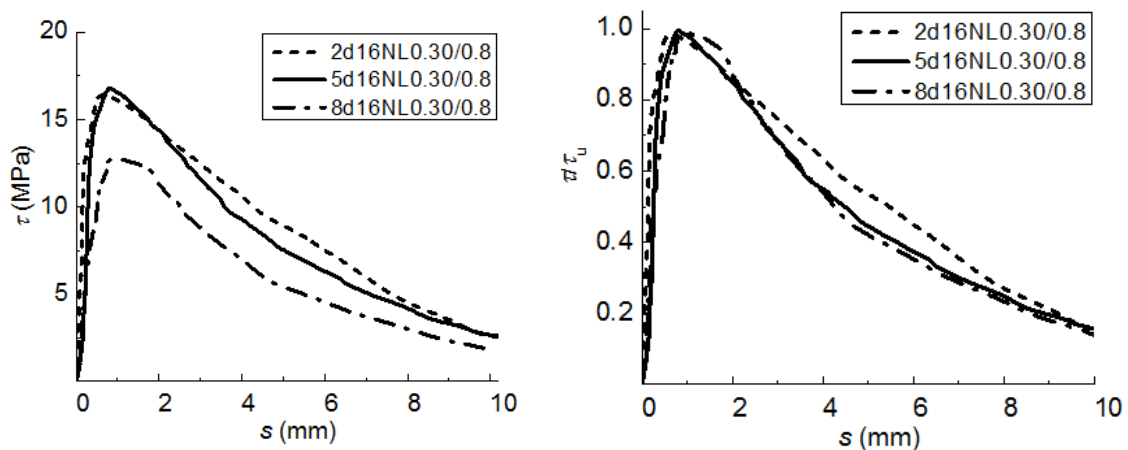


Fig. 8 - Bond stress-slip curves and bond sustainability affected by bond length of rebar

The above differences may be concluded to the different bond mechanism affected by bond length. As the rib space is about $0.7d$, the number of ribs took part in the bearing action is about 3, 7 and 11 corresponding to the rebar with $2d$, $5d$ and $8d$ bond length. Because of the transfer of bond slip from loading-end to free-end, the bearing action of ribs took place successively from the one near the loading-end. For the rebar with $2d$ bond length, the bearing action of ribs could be simultaneous easily and led the bond stress upto the ultimate; after that, the slip increased with the crushing deformation of SFRLAC in front of ribs and the complete shear failure of coarse expanded shales in a plain along the bond length. This exhibited that the even distribution of bond stress along the bond length and the straight reduction of bond stress in descending portion.

For the rebars with $5d$ and $8d$ bond length, the much more number of ribs gave the opportunity of the redistribution of bond stress along bond length with the transfer of slip from

loading-end to free-end [17-20, 26], which let the SFRLAC work successively into effective states. In this condition, the bond reliability was higher because the ribs seceded bearing action one by one with the increasing slip, the obvious reduction of bond stress gave the forebode to avoid related damages.

CONCLUSION

In the test, multi-factors were considered to study their effects on the bond performance of deformed rebar in high-performance SFRLAC. The complete bond stress-slip curves of specimens are obtained by using modified pull-out test with the detection of the slips at loading-end and free-end. The compressive and splitting tensile strength of SFRLAC were also tested. Based on the analyses of test results, the conclusion can be drawn as follow:

- (1) Three kinds of actions affected the bond performance of deformed rebar in high-performance SFRLAC: the adhesion referred to the chemical bonding of set cement, the friction arising from the roughness of the interface and the bearing action due to the anchorage of ribs against SFRLAC surface. To completely and reasonably evaluate the bond behaviours, the differential of bond slip between loading-end and free-end, the bond failure mode and the bond stress-slip curve characterized by bond strength, peak-slip and bond sustainability are analysed.
- (2) Steel fibers in LAC benefited to the ductile failure of bond test specimens by altering the failure mode from splitting to pull-out. The width of cracks appeared on surface of SFRLAC specimens decreased obviously with the increase of volume fraction of steel fiber. When the bond length reached $11d$, the fracture of rebar took place without failure of SFRLAC specimens.
- (3) The strengthening effect of steel fiber on bond strength is lower than that on tensile strength. With the increase of volume fraction of steel fiber, the peak-slips were almost equal while the deviation of slips at loading-end and free-end increased, the bond sustainability in descending portion was improved. When the volume fraction of steel fiber was no less than 0.8%, the bond sustainability was higher with the ductile bond failure.
- (4) The bond performance was improved by decreasing the water-cement ratio. The bond strength increased, the mean values of peak-slip were almost equal with the greater differential of slips at loading-end and free-end. The bond sustainability was almost equal when the water-cement ratio was 0.25 and 0.30, while the lower one was for the water-cement ratio of 0.35.
- (5) Compared the bond strength of rebar $d=12\text{mm}$, the bond strength of rebar $d=16\text{mm}$ and 20mm decreased for 2.31% and 5.78%. With the increase of rebar diameter, the mean value of peak-slip decreased with the reduced differential of slips between loading-end and free-end, the bond sustainability reduced. Except the difference of rebar dimension, the different concrete cover should be considered.
- (6) The higher strength of coarse expanded shale led to the higher bond strength, the larger differential of slip between loading-end and free-end and the higher bond sustainability. The effect of fine expanded shale replaced by manufactured sand on bond performance could be eliminated.
- (7) The bond strength of rebar with $2d$ bond length was equal to that with $5d$ bond length, while the bond strength of rebar with $8d$ bond length was lower about 30%. The rebars with $5d$ and $8d$ bond length presented the similar bond stress-slip curve and bond sustainability, while the better behaviors was exhibited for the rebar with $2d$ bond length. Meanwhile, the bond sustainability of rebar with $8d$ bond strength at the initial part of descending portion was greater, which provided a higher reliability to sustain the bond strength with a greater peak-slip.

ACKNOWLEDGEMENTS

This study was financially supported by the NCWU Innovation Funds for Doctoral Candidate (201714402), the Key Research Project in University of Henan Province, China (14B560004, 16A560024), and the Science and Technology Innovation Team of Eco-building Material and Structural Engineering in University of Henan Province, China (13IRTSTHN002) .

REFERENCES

- [1] JGJ12, 2006. Design Specification for Lightweight Aggregate Concrete Structures (China Building Industry Press) 62 pp.
- [2] CECS 202:2006, Technical Specification for Lightweight Aggregate Concrete Bridges, China Plan Press, Beijing, China, 2006.
- [3] Zhao M.S., Ma Y.Y., Pan L.Y., Li C.Y., 2015. An overview of study on natural lightweight aggregate for concrete in China. In: 3rd International Conference on Civil Engineering, Architecture and Sustainable Infrastructure, Edited by Zhang X.Q., Zhao S.B. & Xie Y.M., DEStech Publications, Inc., 125-133
- [4] Hassanpour M., Shafigh P., Mahmud H.B., 2012. Lightweight aggregate concrete fiber reinforcement –A review. *Construction and Building Materials*, No. 37: 452-461
- [5] Zhao S.B., Li C.Y., Qian X.J., 2011. Experimental study on mechanical properties of steel fiber reinforced full lightweight concrete. *Geotechnical Special Publication*, No. 212: 233-239
- [6] Pan L.Y., Yuan H., Zhao S.B., 2011. Experimental study on mechanical properties of hybrid fiber reinforced full lightweight aggregate concrete. *Advanced Materials Research*, Vol. 197-198: 911-914
- [7] Shen Z., Chen M.H., Zhao M.S., Li X.K., 2015. Experimental study on tensile properties of steel fiber reinforced lightweight-aggregate fly-ash flowable concrete. In: *Architectural Engineering and New Materials*, Edited by Badorul H.A.B., Meor O.H. & Noridah M., DEStech Publications, Inc: PA, USA, 1-8
- [8] Li X.K., Zhang X.Y., Li M.Q., Zhao M.S., Li C.Y., 2017. Experiments on development of strength and carbonization of steel fiber reinforced full-lightweight concrete. *Journal of Civil Engineering and Management*, Vol. 34, No. 2: 46-50
- [9] Zhao S.B., Li C.Y., Zhao M.S., Zhang X.Y., 2016. Experimental study on autogenous and drying shrinkage of steel fiber reinforced lightweight-aggregate concrete. *Advances in Material Science and Engineering*, Vol. 2016, Article ID2589383, pages 10
- [10] Li C.Y., Zhao S.B., Chen H., Gao D.Y., Ding X.X., 2015. Experimental study on flexural capacity of reinforced SFRFLC superposed beams. *Journal of Building Structures*, Vol. 36, Suppl. 2: 257-264
- [11] Li C.Y., Ding X.X., Zhao S.B., Zhang X.Y., Li X.K., 2016. Cracking resistance of reinforced SFRFLC superposed beams with partial ordinary concrete in compression zone. *The Open Civil Engineering Journal*, No. 10: 727-737
- [12] Pei S.W., Du Z.H., Li C.Y., Shi F.J., 2013. Research of punching performance of reinforced SFRLAC superposed two-way slabs. *Applied Mechanics and Materials*, Vols. 438-439: 667-672
- [13] Mo K.H., Alengaram U.J., Jumaat M. Z., 2016. Bond properties of lightweight concrete -A review. *Construction and Building Materials*, No. 112: 478-496
- [14] Li F.L., Yu Y.N., Yu K.F., Chen J.Q., 2014. Experimental study on bond properties of plain steel bar with SFRLAC. *Journal of Hebei University of Technology*, Vol. 43, No. 6: 93-96
- [15] Clarke J.L., Birjandi F.K., 1993. Bond strength tests for ribbed bars in lightweight aggregate concrete. *Magazine of Concrete Research*, Vol. 45, No. 163: 79-87
- [16] Konig G., Dehn F., Holschemacher K., Weibe D., 2002. Determination of the bond creep coefficient for lightweight aggregate concrete (LWAC) under cyclic loading. In: *Concrete for Extreme Conditions. Proceedings of the International Conference Held at the University of Dundee, Scotland, UK*, 673-683
- [17] Lachemi M., Bae S., Hossain K. M. A., Sahmaran M., 2009. Steel-concrete bond strength of lightweight self-consolidating concrete. *Materials and Structures*, No. 42: 1015-1023
- [18] Wu X., Wu Z., Zheng J., Zhang X., 2013. Bond behavior of deformed bars in self-compacting lightweight concrete subjected to lateral pressure. *Magazine of Concrete Research*, Vol. 65, No. 23: 1396-1410

- [19] Wei J., Ma J., Yue J., 1993. Experimental study of bond and anchorage of concrete and deformed bars. *Journal of Harbin Architecture & Civil Engineering Institute*, Vol. 26, No. 1: 95-100
- [20] Lu C., Wang W., Li P., 2007. Experimental research on bond behavior between deformed bar and lightweight concrete. *Journal of Guangxi University (Nat Sci Ed)*, Vol. 32, No. 1: 6-9
- [21] Zhang D., Yang W., 2015. Experimental research on bond behaviors between shale ceramsite lightweight aggregate concrete and bars through pullout tests. *Journal of Materials in Civil Engineering*, Vol. 27, No. 9, Article ID 06014030
- [22] Gu C., Zheng X., Zhang W., Chang H., 2017. Test research on bond properties between reinforcing bar and lightweight aggregate concrete. *Journal of Railway Science and Engineering*, Vol. 14, No. 3: 528-535
- [23] Ali A., Iqbal S., Holschemacher K., Bier T., 2016. Effect of fibers on bond performance of lightweight reinforced concrete. *Periodica Polytechnica: Civil Engineering*, Vol. 60, No. 1: 97-102
- [24] Guneyisi E., Gesoglu M., Ipek S., 2013. Effect of steel fiber addition and aspect ratio on bond strength of cold-bonded fly ash lightweight aggregate concrete. *Construction and Building Materials*, No. 47: 358-365
- [25] Campione G., Cucchiara C., Mendola L., Papia M., 2005. Steel-concrete bond in lightweight fiber reinforced concrete under monotonic and cyclic actions. *Engineering Structures*, Vol. 27, No. 6: 881-890
- [26] Zhang H., Lv Z., Liu Y., 2016. Experimental research on bond behavior between steel fiber reinforced high-strength ceramsite concrete and rebar. *Building Structure*, Vol. 46, No. 4: 79-84
- [27] Mo K.H., Goh S.H., Alengaram U.J., Visintin P., Jumaat M.Z., 2017. Mechanical, toughness, bond and durability-related properties of lightweight concrete reinforced with steel fibers. *Materials and Structures*, No. 50:46, pages 14
- [28] JGJ 21, 2002, Technical Specification for Lightweight Aggregate Concrete (China Building Industry Press) 52 pp.
- [29] JG/T 472, 2015. Steel Fiber Reinforced Concrete (China Standard Press) 16 pp.
- [30] GB 50152, 2012. Standard for Test Method of Concrete Structures (China Building Industry Press) 26 pp.
- [31] Zhao S.B., Ding X.X., Li C.M., Li C.Y., 2013. Experimental study on bond properties between deformed steel bar and concrete with machine-made sand. *Journal of Building Materials*, Vol. 12, No. 3: 191-196
- [32] Li C.Y., Zhao M.L., Ren F.C., Liang N., Li J., Zhao M.S., 2017. Bond Properties between full-recycled-aggregate concrete and deformed steel bar. *The Open Civil Engineering Journal*, Vol. 11: 685-698
- [33] GB/T 50081, 2002. Standard for Test Method of Mechanical Properties on Ordinary Concrete (China Building Industry Press) 28 pp.